Defects and welds detection and classification approach based on CNN for oil pipeline MFL data

Iurii Katser, Viacheslav Kozitsin, Ivan Maksimov

Skolkovo Institute of Science and Technology

Abstract

Keywords: deep learning, computer vision, convolutional neural networks, anomaly detection, fault detection, oil pipelines, defects, welds

1. INTRODUCTION

Anomaly detection problems have a great importance in industrial applications, because anomalies usually represent faults, failures or the emergence of such. To detect these automatically, advanced analytic algorithms, including machine learning- and deep learning-based, can be applied. In this work, we investigate deep neural network performances in providing hindsight in oil pipeline diagnostics. This system spans over thousands of kilometers, which makes manual inspection very costly and sometimes impossible. The damage of pipelines that transport petroleum and gas products lead to severe environmental problems. Eliminating breakthroughs and their consequences is expensive. To avoid accidents, it is recommended to improve diagnostics quality and to increase the frequency of in-line-inspection (ILI) tools deployment. ILI tools, also referred to as pipeline inspection gauges (Fig. 1), use Hall effect for measuring localized Magnetic Flux Leakage (MFL) intensity along the pipe wall. While moving along the pipe gauge inspects the wall and detects the magnetic field leaks. MFL technique is the most common approach for oil and gas pipelines nondestructive testing nowadays. The data

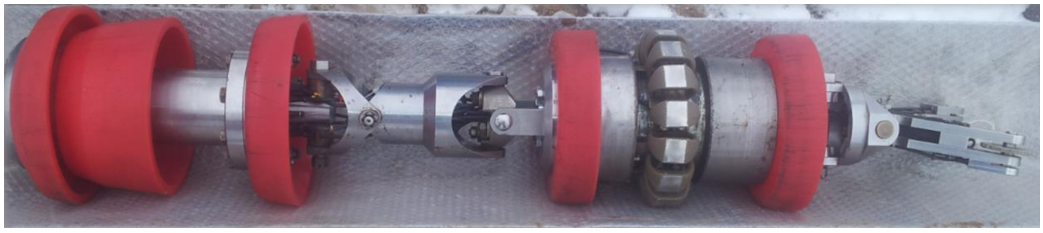

Figure 1: In-line-inspection tool

collected during the inspection can be further analyzed for main diagnostics problems solving: damage and defects detection, their localization, diagnosis or defects classification. Analysis results are useful for assets managing and repair priorities determination.

There are three main classes of data that are attended to by diagnostics personnel. They are presented in Fig. 2. Some other classes of data (pipe tee, bend) are out of the scope of this work just like different classes of defects.

The rest of the paper is devoted to appraising computer vision (CV) techniques proficiency in oil pipeline diagnostics application.

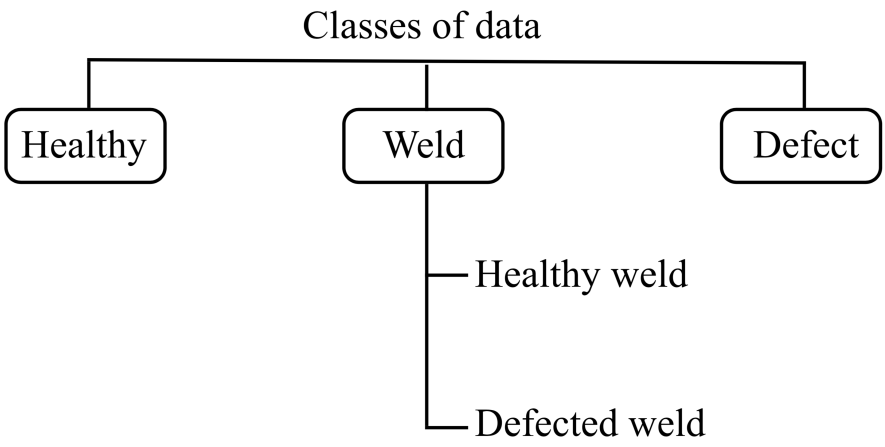

Figure 2: Image classes that are distinguished in the work

2. LITERATURE REVIEW

2.1. Pipelines defects diagnostics

Magnetic Flux Leakage (MFL) technique is the most common approach for oil and gas pipelines nondestructive testing. The data obtained during the pipeline inspection process is primarily analyzed by traditional machine learning (ML) methods. A comparison of performance among different ML methods for defects identification problem is presented in [1]. The main challenge for this approach is creating informative and important features that will be used as an input for ML methods. Usually, these diagnostics features are generated using expert knowledge and manually-created heuristics. It imposes the limitation on defects detection problem solving quality. A variety of most successful features is presented and analyzed in details in [2].

Deep Learning showed significant progress and achieved incredible results in numerous applications, just in the past few years. The image classification problem is one of the most successful applications of DL and Convolutional Neural Networks (CNNs) in particular. To automate the process of feature generation in MFL data analysis, CNNs can be used either. As an advantage, they can solve the defects or welds detection, classification and segmentation problems at the same time. In literature there are examples of applying CNNs for defects detection [3], welds defect detection [4], welds and defects classification [5], defect size estimation [6]. For all mentioned applications, CNNs outperformed existing traditional approaches. Nevertheless, still, there are just a few works dedicated to MFL data analysis using DL. A number of particular problems that can be solved using a novel approach are not covered yet. For instance, we could not find any works on applying CNNs to defects segmentation task, despite the importance of this problem solving according to [3].

In this work, we want to research two different problems:

1. Defects detection (Picture classification task).
2. Defects segmentation (Semantic segmentation task).

For their solving, we propose CNNs of different architectures and compare their results with existing state-of-the-art approaches. Moreover, we research different preprocessing techniques for dealing with typical issues in the MFL data.

2.2. Unet

asd [7]

3. DATASET DESCRIPTION AND PREPROCESSING PROCEDURES

Although MFL data looks quite similar for different pipes and ILI tool types, it can differ significantly. The data mainly depends on pipe size, wall width, sensors geometry, and other geometric characteristics. Moreover, ILI tools differ a lot for different pipe sizes. Therefore, the repeatability of the results for different datasets should be investigated additionally. Following, we provide dataset characteristics, which are also presented in Table 1. We have data collected from the 219 mm in diameter pipe. MFL dataset provides information about a single inspection tool run. Dataset has 64 features collected as an array with a constant step along with the ILI tool movement inside the pipe. Dataset has 4470704 samples that represent 15162.85 meters long pipeline part. Sample values vary from 0 to 4095 units. It has 745 defects of different types and 1462 welds, 34 of which are defected. Fig. 3 shows examples of healthy data, data with a weld, and with a defect. Attached to the dataset technical report contains information about welds and defects location, defects types, sizes, and other related characteristics.

Table 1: Dataset characteristics.

Parameter	Value
Pipeline diameter, mm	219
Pipeline length, m	15162.85
Number of samples	4470704
Number of features	64
Min value	0
Max value	4095
Mean value	
Number of defects/welds	745/1462

Raw data has several issues that don't allow us to solve CV problems without proper preprocessing. They are:

1. Sensors malfunctions (zeroed values cause bold horizontal line in Fig. 3);
2. Displaced origins between data and reports coordinates;
3. Inaccurate annotations, e.g., missed defects, wrong defect location, etc.
4. No annotated data for the segmentation task.

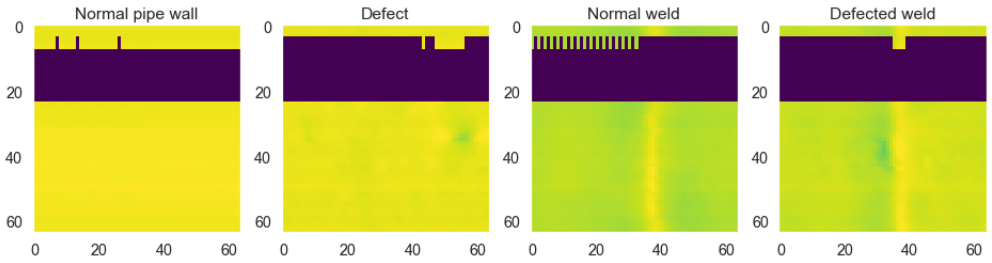

Figure 3: Example of the MFL data

3.0.1. Sensors malfunctions problem

To deal with sensors malfunctions we suppose to fill the gaps (zeroed values) with values calculated by different methods. Additionaly, we will consider values less than 2000 abnormal and replace them with zeroes during the preprocessing.

1. Abnormal values are equal to 0. Then Min-Max scaling to $[0.5 : 1]$ range.
2. Abnormal values are equal to the mean of normal values from one picture. Then Min-Max scaling.
3. Abnormal values are equal to the mean of normal values over the column. Then Min-Max scaling.
4. Abnormal values are equal to the mean of neighboring sensors over the column. Then Min-Max scaling.
5. Abnormal values are equal to the interpolation results over the column. Then Min-Max scaling.
6. Rerange initial set of values to 0...255 uint8 range.
7. Rerange initial set of values to 0...1 float range
   (Fig. 4). Such a specific function due to the range of normal operation of the sensor from 2500 to 3500 units.

The results of all applied methods are presented in Fig. 5.

Min-Max scaling can be applied using whole dataset or just one image. Both approaches will be compared during the experiment conducting.

Since the ILI tool location data did not match the defect location data from the report, it was necessary to merge the data. The key factor here turned out to be that signal values from magnetic flux sensors grow at the weld site (Figure 6).

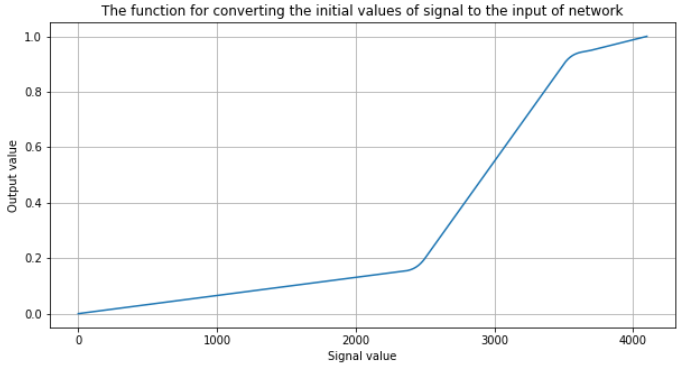

Figure 4: The function for converting the initial values of signal to the input of network

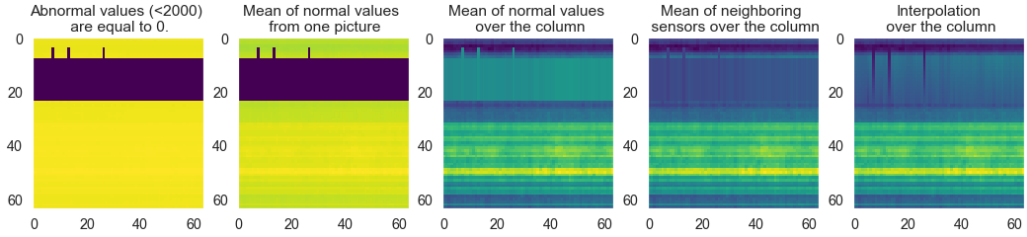

Figure 5: Comparison of methods for missing values filling

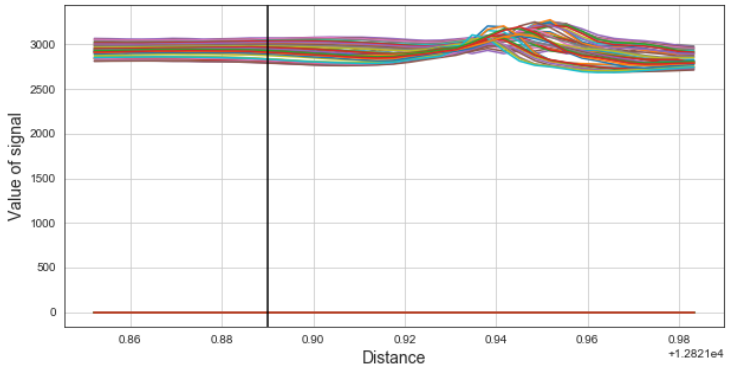

Figure 6: Location of a weld. The black vertical line is a weld, according to the report. Other lines are values from sensors.

The solution was to find the locations of the maxima of sensors data values and then to combine it with the weld coordinates.

3.0.2. Manual annotations for the segmentation task

Since there was no annotated data for the segmentation problem, it was necessary to annotate it manually (Figure 7). The characteristics of the obtained dataset can be seen in Table 3.

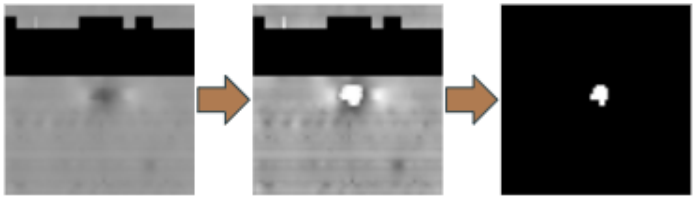

Figure 7: The methodology for obtaining the mask

3.0.3. Inaccurate annotations problem

This problem is a common one for oil and gas pipeline nondestructive testing [1]. It appears to be a lot of missing defects that affect the quality of the problem. Besides, there are wrong defect types and locations. To eliminate wrong location issue, we additionaly searched extremums around the provided location and chose the defects or welds taking into account new coordinates.

3.0.4. Augmentation

Although we have a lot of data, we don't have a lot of defects and welds in comparison with healthy pipe wall instances. We use the augmentation procedure to balance classes of pictures and increase the model's quality by increasing the number of pictures in small classes (defects, welds). As an augmentation tool we use Albumentations library [8]. All applied augmentations both for welds and defects are presented in Table 2. Applied augmentations details are presented in [8] and references therein.

Examples of augmentations are shown in Fig. 8.

The characteristics of the pipeline defects dataset are described in Table 3, where * symbol indicates a random call function 5 and 6 from the defects augmentation list, so the exact number is unknown.

Table 2: Applied augmentations.

Augmentation Types	Pipelines (welds)	Pipelines (defects)
Rotate90	-	✓
Rotate180	✓	✓
Rotate270	-	✓
VerticalFlip	✓	✓
HorizontalFlip	✓	✓
ElasticTransform	✓	✓
GridDistortion	✓	✓
OpticalDistortion	✓	✓
Transpose	-	✓
RandomRotate90	-	✓

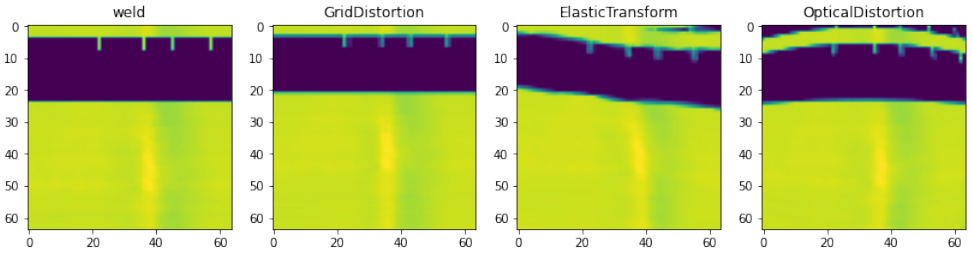

Figure 8: Examples of the augmented weld image

Table 3: Dataset size for pipeline defects detection and segmentation problems

	Classification			Segmentation	
Data	Healthy	Defect	Weld	Healthy	Defect
Before augmentation					
Train	11106	569	1130	181	450
Validation	584	142	282	33	111
After augmentation					
Train	11106	8535	11300	*	*
Validation	584	142	282	*	*

4. METHODS

Pipeline defect detection is composed of two problems. First, the defect should be detected, and further, it should be evaluated using segmentation

results. We propose here a novel CNN architecture for image classification. Additionally, we present the existing architectures that achieve best results in the MFL and X-ray data classification problems.

4.1. CNN Preliminaries

A CNN is a special type of a neural network that has proven effective in computer vision applications. State-of-the-art results can be achieved in segmentation and classification tasks [**?**]. Compared to computer vision algorithms that do not take advantage of CNNs, much less pre-processing is required. More importantly, such networks are able to learn characteristics from data, which otherwise would have to be individually accounted for [**?**].

Even though CNNs have been proposed in different architectures - to increase their efficiency for specific tasks and/or datasets, three different types of layers are used without exception, each with a specific propose: convolutional, pooling, and fully connected (linear) layers. The convolutional layers aim to extract feature maps of the input images by applying filters over different region of images. For instance, with k filters, each filter having weight and bias of w_i and b_i, respectively, the convolution of an image patch, x_n, can be written as follows:

$$f_{i,n} = \sigma(W_i x_n + b_i), \tag{1}$$

where σ is the activation function. Besides rectified linear units (ReLU), sigmoid or softmax activation functions, a multitude of different options exist, all having their individual advantages. These are applied on a layers's output neurons (e.g. after a convolutional layer). After a number of convolutional layers, pooling layers are commonly applied in prominent network architectures to reduce the size of particular dimensions. Max-pooling and average-pooling are two examples. Pooling layers, alongside reducing dimensions's sizes, perform denoising when utilized on images. Fully connected layers are generally the last layers of CNNs, possessing a similar structure compared to the traditional neural networks[**?**].

4.2. CNN Structure

Proposed model (Fig. 9) consists of 5 Convolutional layers overall. Each Convolutional layer is followed by BN and Dropout sequentially (not shown in Fig. 9). All Convolutional layers have equal kernel size - 5 x 5. All MaxPooling layers have equal kernel size - 2 x 2, and stride - 2. From now on this CNN is marked as CNN-5.

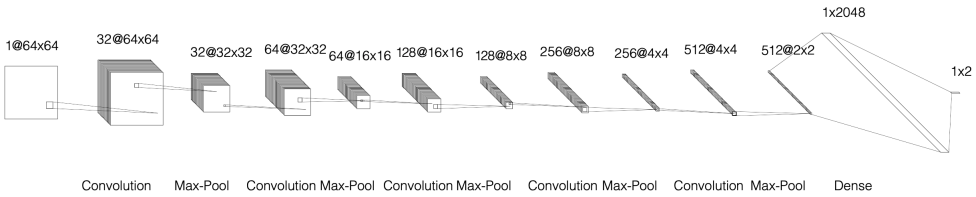

Figure 9: Architecture of the proposed CNN

4.3. Performance metrics

For the classification problem we use Accuracy. Accuracy is defined by the formula:

$$Acc = \frac{\sum_{i=0}^{N} 1_{\{\hat{y}_i = y_i\}}}{N} \tag{2}$$

where N - number of samples, $\hat{y}$ - predicted label, y - true label.

4.4. Loss functions

Weighted Binary Cross-Entropy both for segmentation and detection problems:

$$wBCE = -\frac{1}{N}\sum_{i=1}^{N} w_1 \cdot y_i \cdot \log\left(p\left(\hat{y}_i\right)\right) + w_2 \cdot \left(1 - y_i\right) \cdot \log\left(1 - p\left(\hat{y}_i\right)\right) \tag{3}$$

4.5. Existing CNNs

We reimplemented CNN from [3] with one difference: we used squared pictures (64x64 pixels) as an input, so we didn't implement Normalization layer (first layer in the Fig. 10). The interested reader can find all details

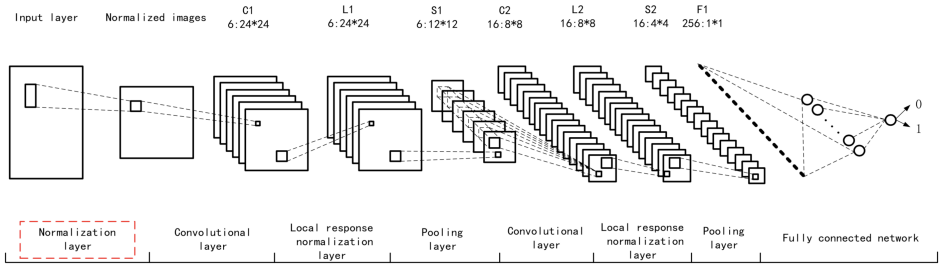

Figure 10: Architecture of CNN from [3]

and overall architecture parameters in [3]. From now on this CNN is marked as CNN-2 by the number of Convolutional layers.

We also reimplemented CNN from [4], which showed better results than pre-trained and fine-tuned OverFeatNet, VGGNet, GoogleNet networks. The architecture is shown in Fig. 11. Since our input size is smaller than in the original paper, we used smaller kernel size (3x3 instead of 7x7). All details

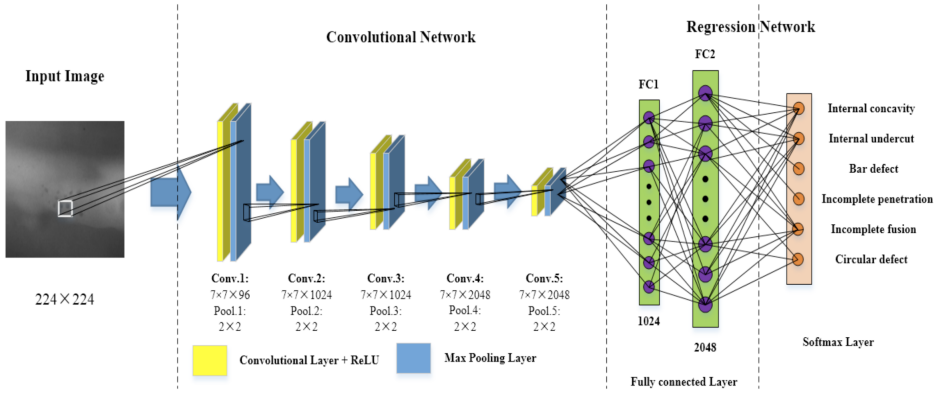

Figure 11: Architecture of CNN from [4]

and CNN's parameters are presented in [4]. From now on this CNN is marked as RayNet.

5. RESULTS

We present the results of comparison for different preprocessing techniques and different CNN architectures for binary classification (normal pipe wall or defect/weld) in Tab. 4 and multiclass classification problem (normal pipe wall, defect or weld) in Tab. 5.

Batch size is equal to 64, so the input to the network has shape (64, 1, 64, 64). For all experiments, we use Adam optimizer with initial learning rate 0.001 and learning rate scheduler with parameters: threshold = 0.0001, factor = 0.5, min lr = 0.0001, patience = 484. Also, for all experiments, the number of epochs is equal to 12. Dropout rate for all experiments is equal to 0.33. All mentioned parameters were selected by using grid search procedure.

Table 4: Comparison of performance among different classification methods for binary classification problem. $\hat{y} = y = 0$ - healthy; $\hat{y} = y = 1$ - defect/weld.

Method	$\hat{y} = y = 0$	$\hat{y} = y = 1$	Average
CNN-2	95.55	82.08	89.88
RayNet			
CNN-5	97.95	**91.51**	**95.24**
CNN-5+LRN	**98.29**	89.86	94.74
Filling techniques comparison			
CNN-5 (filling 1)	97.95	**91.51**	**95.24**
CNN-5 (filling 2)	97.95	84.20	92.16
CNN-5 (filling 3)	97.26	83.02	91.27
CNN-5 (filling 4)	**98.63**	81.13	91.27
CNN-5 (filling 5)	98.12	81.84	91.27

Filling methods were researched for binary classification problem. Centering means using peaks (extremums) searching procedure for welds or defects correct coordinates defining. The centering procedure was research both for binary and multiclass classification problems. Moreover, Min-Max normalization with using either a single image or whole dataset was investigated. Finally, CNN-2 and CNN-5 were compared for centered images with the first filling method using single image Min-Max normalization.

Table 5: Comparison of performance among different classification methods for multiclass classification problem. $\hat{y} = y = 0$ - healthy; $\hat{y} = y = 1$ - defect; $\hat{y} = y = 2$ - weld.

Method	$\hat{y} = y = 0$	$\hat{y} = y = 1$	$\hat{y} = y = 2$	Average
CNN-2	97.60	59.86	92.91	90.97
RayNet				
CNN-5	**98.12**	**76.76**	**98.23**	**95.14**
Single image normalization vs Whole dataset normalization				
CNN-5 (1) (whole)	97.95	64.08	**99.65**	93.65
CNN-5 (1) (image)	98.12	**76.76**	98.23	**95.14**
CNN-2 (1) (whole)	**99.32**	13.38	96.45	86.41
CNN-2 (1) (image)	97.60	59.86	92.91	90.97
CNN-5 (3) (whole)	99.66	81.69	99.65	97.12
CNN-2 (3) (whole)	95.72	13.38	97.52	89.58

6. CONCLUSION

Today, manual analysis of a magnetographic image is being a bottleneck for the diagnosis of pipelines, since it costs a lot of money and is limited by human resources. This study allows us to hope that this process can be fully automated, which is likely to make the analysis more reliable, faster and cheaper.

The network (CNN-5) that outperformed currently used CNNs for defect detection of pipelines was proposed. Moreover, we proposed a modified UNet for defects of pipelines segmentation. The results of segmentation show the applicability of the proposed UNet for the size of defects evaluation. The results of the experiments prove that all parts of the oil pipeline diagnostics process can be fully automated with high quality.

Finally, there can be defined several project development options:

1. increasing sizes of the datasets;
2. improving preprocessing procedures, including manual pictures selection;
3. multiclass defects classification for pipelines dataset;
4. defected and healthy welds classification for pipelines dataset;
5. defect depth evaluation for pipelines dataset;
6. investigate the repeatability of the results for similar datasets.

[1] A. Khodayari-Rostamabad, J. Reilly, N. Nikolova, J. Hare, S. Pasha, Machine learning techniques for the analysis of magnetic flux leakage images in pipeline inspection, IEEE Transactions on Magnetics 45 (8) (2009) 3073–3084. doi:10.1109/tmag.2009.2020160.

[2] S. D.A., Development of the magnetic method of non-destructive testing due to automation of data processing and optimization of defect detection algorithms, Ph.D. thesis, National Research University "Moscow Power Engineering Institute" (2017).

[3] J. Feng, F. Li, S. Lu, J. Liu, D. Ma, Injurious or noninjurious defect identification from MFL images in pipeline inspection using convolutional neural network, IEEE Transactions on Instrumentation and Measurement 66 (7) (2017) 1883–1892. doi:10.1109/tim.2017.2673024.

[4] Oil pipeline weld defect identification system based on convolutional neural network, KSII Transactions on Internet and Information Systems 14 (3) (mar 2020). doi:10.3837/tiis.2020.03.010.

[5] L. Yang, Z. Wang, S. Gao, Pipeline magnetic flux leakage image detection algorithm based on multiscale SSD network, IEEE Transactions on Industrial Informatics 16 (1) (2020) 501–509. doi:10.1109/tii.2019.2926283.

[6] S. Lu, J. Feng, H. Zhang, J. Liu, Z. Wu, An estimation method of defect size from MFL image using visual transformation convolutional neural network, IEEE Transactions on Industrial Informatics 15 (1) (2019) 213–224. doi:10.1109/tii.2018.2828811.

[7] O. Ronneberger, P. Fischer, T. Brox, U-net: Convolutional networks for biomedical image segmentation, in: Lecture Notes in Computer Science, Springer International Publishing, 2015, pp. 234–241. doi:$10.1007/978-3-319-24574-4_28$.

[8] A. Buslaev, V. I. Iglovikov, E. Khvedchenya, A. Parinov, M. Druzhinin, A. A. Kalinin, Albumentations: fast and flexible image augmentations, Information 11 (2) (2020) 125.